Inorganica Chimica Acta 429 (2015) 227–236

Contents lists available at ScienceDirect

Inorganica Chimica Acta

journal homepage: www.elsevier.com/locate/ica

Dithiocarbamate copper(I) and silver(I) complexes: Synthesis, structure and thermal behavior

Robert Mothes, Holm Petzold, Alexander Jakob, Tobias Rüffer, Heinrich Lang *

Technische Universität Chemnitz, Faculty of Natural Sciences, Institute of Chemistry, Inorganic Chemistry, 09107 Chemnitz, Germany

ARTICLE INFO

Article history:
Received 11 December 2014
Received in revised form 2 February 2015
Accepted 5 February 2015
Available online 20 February 2015

Keywords:
Metal
Metal sulfide
Dithiocarbamate
Dynamic NMR spectroscopy
Thermal decomposition

ABSTRACT

Complexes $[M(PBu_3)_n(S_2CNRR')]$ (M = Cu, Ag; n = 1, 2, 3; R = R′ = $CH_2CH{=}CH_2$, $(CH_2)_4$, C_2H_4OH; R = Me, R′ = C_2H_4OH; R = Bu, R′ = C_2H_4OH) (**4**–**9**) are accessible by the reaction of $[Cu(PBu_3)_nCl]$ (**1a**–**c**) or $[Ag(PBu_3)_n(NO_3)]$ (**2a**–**c**) with $[K(S_2CNRR')]$ (**3a**–**e**). The respective silver(I) dithiocarbamates **7**–**9** and $[Ag(PPh_3)_2(S_2CNRR')]$ (**12a**, R = Me; **12b**, R = Bu) could be synthesized by the subsequent treatment of **3** with $[AgNO_3]$ (**10**) giving $[AgS_2CNRR']$ (**11**) followed by addition of n equivalents of the phosphine L (L = PBu_3, PPh_3). Exemplary, the $^{31}P\{^1H\}$ NMR spectra of $[Ag(PBu_3)_n(S_2CNMe(C_2H_4OH)]$ (n = 1.0, 1.5, 2.0, 2.5, 3.0, 3.5, 4.0, 4.5) were investigated in the temperature range of 308–178 K showing phosphine ligand exchange processes in solution. The molecular structures of **12a**,**b** in the solid state are reported confirming the monomeric architecture with coordination number 4 at silver, which is setup by a chelate-bonded (κ^2-S,S′) $S_2CNR(C_2H_4OH)$ unit and two coordinated PPh_3 ligands. The thermal behavior of selected samples was studied by thermogravimetry. Depending on R, R′ and the number of phosphines n, decomposition occurs in varying temperature ranges giving different decomposition residues (Cu_xS, x = 1.96, 2; Ag, Ag_2S), which were characterized by XRPD.

1. Introduction

Dithiocarbamate-containing coordination compounds represent a class of transition metal complexes, which are accessible by using different synthetic methodologies [1]. Over the last decades, a versatile chemistry has been developed around them and a wide-ranging field of applications including analytical chemistry [2], material sciences [3], homogeneous catalysis [4], and biology [5] has been established. The enormous interest in dithiocarbamate compounds results from their ability to coordinate different metals in diverse bonding modes [1,6], which, for example, allows the simultaneous determination of copper and silver in wastewater [7]. For all applications, consolidated knowledge of the coordinating behavior of the respective dithiocarbamates complexes is of prime importance. Though, with exclusion of limited examples, the interaction between copper(I) and/or silver(I) dithiocarbamates and phosphines regarding spectroscopic and structural features is only rarely described in literature [8]. Hence, we got interested in the investigation of the interaction between selected copper(I) and silver(I) dithiocarbamates with phosphines PR_3 (R = Bu, Ph) and their use as precursors in deposition processes.

Herein, we discuss the synthesis, properties, characterization, and thermal behavior of a series of phosphine copper(I) and silver(I) dithiocarbamate complexes of structural type $[ML_n(S_2CNRR')]$ (M = Cu, Ag; L = PBu_3, PPh_3; n = 1, 2, 3; R = R′ = $CH_2CH{=}CH_2$, $(CH_2)_4$, C_2H_4OH; R = Me, R′ = C_2H_4OH; R = Bu, R′ = C_2H_4OH).

2. Results and discussion

Phosphine copper(I) and silver(I) dithiocarbamate complexes of type $[M(PBu_3)_n(S_2CNRR')]$ (M = Cu, Ag; n = 1, 2, 3; R = R′ = $CH_2CH{=}CH_2$, $(CH_2)_4$, C_2H_4OH; R = Me, R′ = C_2H_4OH; R = Bu, R′ = C_2H_4OH) (**4**–**9**) have been prepared by reacting $[Cu(PBu_3)_nCl]$ (**1a**–**c**) or $[Ag(PBu_3)_n(NO_3)]$ (**2a**–**c**) with $[K(S_2CNRR')]$ (**3a**–**e**) as shown in Scheme 1 (Table 1). The potassium dithiocarbamate salts **3a**–**e** were accessible by treatment of the secondary amines diallylamine, pyrrolidine, diethanolamine, 2-(methylamino)ethanol, or 2-(butylamino)ethanol with an excess of carbon disulfide in ethanolic potassium hydroxide solutions at 0 °C [9]. Another synthetic methodology to prepare the phosphine silver(I) dithiocarbamates **7**–**9** and additional $[Ag(PPh_3)_2(S_2CNR(C_2H_4OH)]$ (**12a**, R = Me; **12b**, R = Bu) relates upon the subsequent reaction of **3d**,**e** with stoichiometric amounts of $[AgNO_3]$ (**10**) to afford $[AgS_2CNR(C_2H_4OH)]$ (**11a**, R = Me; **11b**, R = Bu) followed by addition of n equivalents of the phosphine PR_3 (n = 1, 2, 3) (Scheme 1)

---

* Corresponding author.

http://dx.doi.org/10.1016/j.ica.2015.02.008
0020-1693/© 2015 Elsevier B.V. All rights reserved.

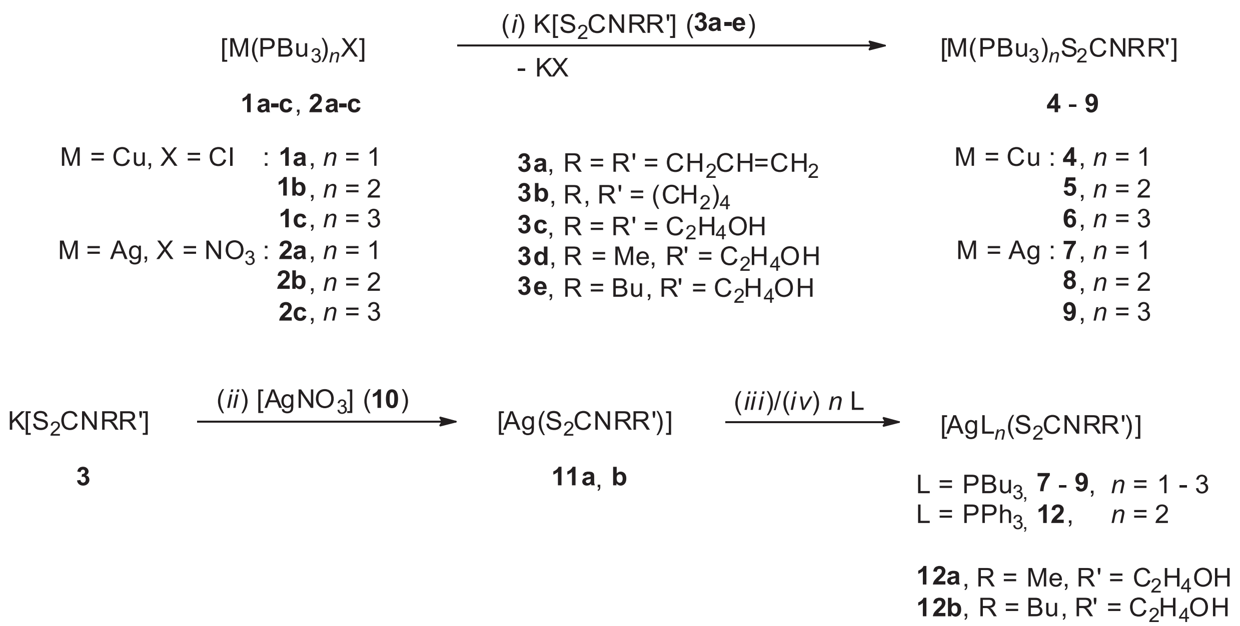

Scheme 1. Synthesis of **4–9**, **11** and **12** (Table 1). ((i) pentane, 0 °C; (ii) acetonitrile/ethanol (ratio 1:50, v/v), 0 °C; (iii) L = PBu_3, pentane, 0 °C; (iv) L = PPh_3, dichloromethane, 25 °C).

Table 1
Complexes $[ML_n(S_2CNRR')]$ (**4–9**, **11** and **12**).

Compd.	M	L	*n*	R	R′	Yield [%][a]
4	Cu	PBu_3	1	C_2H_4OH	Me	93
5a	Cu	PBu_3	2	C_2H_4OH	Me	94
5b	Cu	PBu_3	2	C_2H_4OH	C_2H_4OH	91
5c	Cu	PBu_3	2	$CH_2CH{=}CH_2$	$CH_2CH{=}CH_2$	87
6a	Cu	PBu_3	3	C_2H_4OH	Me	93
6b	Cu	PBu_3	3	C_2H_4OH	C_2H_4OH	90
6c	Cu	PBu_3	3	$CH_2CH{=}CH_2$	$CH_2CH{=}CH_2$	86
6d	Cu	PBu_3	3	$(CH_2)_4$		88
7	Ag	PBu_3	1	C_2H_4OH	Me	92[b]
8a	Ag	PBu_3	2	C_2H_4OH	Me	91[b]
8b	Ag	PBu_3	2	$CH_2CH{=}CH_2$	$CH_2CH{=}CH_2$	88[b]
9a	Ag	PBu_3	3	C_2H_4OH	Me	92[b]
9b	Ag	PBu_3	3	$CH_2CH{=}CH_2$	$CH_2CH{=}CH_2$	86[b]
11a	Ag			C_2H_4OH	Me	96[c]
11b	Ag			C_2H_4OH	Bu	89[c]
12a	Ag	PPh_3	2	C_2H_4OH	Me	93[d]
12b	Ag	PPh_3	2	C_2H_4OH	Bu	96[d]

[a] Based on charged **1a**–**c** or **2a**–**c**.
[b] Reaction pathway (*i*).
[c] Based on charged **3**.
[d] Based on charged **11**.

(Section 4). After appropriate work-up, the PPh_3-based compounds were obtained as solids, while the respective PBu_3-functionalized transition metal complexes are liquids. Further conspicuous is that the appropriate pale yellow copper(I) complexes are sensitive to air- and moisture, while the off-white silver(I) derivatives are stable under similar conditions, however, upon exposure to light they decompose in between days forming elemental silver. The tri-*n*-butylphosphine metal complexes **4–9** are soluble in most common polar and non-polar organic solvents, while the PPh_3 ligands in **12a**,**b** are responsible for the less solubility of these complexes (Section 4).

Complexes **4–9**, **11** and **12** were characterized by elemental analysis, IR and NMR (^1H, $^{13}C\{^1H\}$, $^{31}P\{^1H\}$) spectroscopy (Section 4). The thermal behavior of selected samples was studied by TG (=Thermogravimetry). The molecular structures of **12a**,**b** in the solid state are reported.

The IR spectra of **4–9**, **11** and **12** are characterized by distinct absorptions typical for the dithiocarbamate units with vibrations at ca. 1500 cm^{-1} ($\tilde{\nu}_{C-N}$) and 1000 cm^{-1} ($\tilde{\nu}_{C-S}$) (Section 4) [1]. Generally, the Bonati and Ugo [10] criterion based on the number and splitting of $\tilde{\nu}_{C-S}$ bands at 1050–950 cm^{-1} is used for the differentiation of chelating and monodentate binding modes of dithiocarbamates. More lately, Kellner et al. [11] proposed interligand coupling of the CS ligand as origin of the splitting and hence ruled out the possibility of predicting the dithiocarbamate binding motif from IR vibrations. Nevertheless, the presence of solely one CS band indicates a chelating binding type as also discussed in the dynamic NMR section and the solid state structure (see below).

As expected, the hydroxyl functionality gives rise to a broad band at 3350 cm^{-1}. All vibrations proposed for the phosphine ligand, if present in the respective compound, were found, being only slightly shifted with respect to those of the free donors (Section 4).

^1H NMR spectroscopy allows the assignment of all organic groups present (Section 4). As exemplary shown for $[Ag(PBu_3)_2(S_2CNMe(C_2H_4OH))]$ (**8a**) (Fig. 1), upon decreasing the temperature the resonance signals for the dithiocarbamate functionality are slightly shifted to higher field. The signal corresponding to the OH proton is most affected and shifted to lower field, which is likely caused by the formation of stronger hydrogen-bonds [12].

In addition, $^{13}C\{^1H\}$ NMR spectroscopy can be used for monitoring the progress of the formation of **4–9**, **11** and **12** starting from **3**, which is accompanied by a distinctive shift of the resonance signals of the quaternary dithiocarbamate carbon atoms to higher field (**3a–e**, 214.5–208.0 ppm; **4–9**, **11** and **12**, 213.0–203.7 ppm) (Section 4). The data are in agreement with similar dithiocarbamate transition metal complexes [8a].

The coordination of the phosphine ligands to copper(I) or silver(I) in dithiocarbamates **4–9** and **12** can best be monitored by $^{31}P\{^1H\}$ NMR spectroscopy, since the respective chemical shift gives evidence of the bonding behavior between the phosphorus and the transition metal atom (Section 4) [13]. Additional evidence comes from the $J_{^{107}Ag^{31}P}$ and $J_{^{109}Ag^{31}P}$ coupling constants of the appropriate silver(I) species (Fig. 2). Furthermore, with increasing number of phosphine ligands at silver following trends were observed:

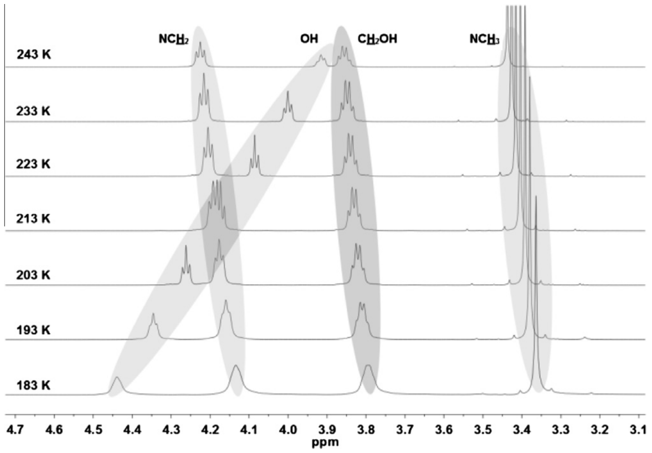

Fig. 1. Cutout of temperature dependent ^1H NMR spectra of [Ag(PBu$_3$)$_2$(S$_2$CNMe(C$_2$H$_4$OH))] (**8a**) in D$_2$-dichloromethane (temperature range: 183–243 K).

(i) the $^{107}Ag–^{31}P$ and $^{107}Ag–^{31}P$ coupling constants decreases and (ii) the resonance signals appear at higher field (Section 4). A typical observation for the silver(I) complexes is the loss of coupling at ambient temperature indicating a fast exchange of the phosphine ligands L on the NMR time scale. This was reported for various copper(I) and silver(I) species of general type [ML$_n$Y]/[ML$_4$][Y] (L = phosphine, phosphite; M = Cu, Ag; n = 1, 2, 3; Y = organic or inorganic group) [13,14]. In order to obtain well-resolved silver–phosphorus coupling patterns the interchange of ligands has to be decelerated. Indeed, low-temperature $^{31}P\{^1H\}$ NMR spectra show the typical two superimposed doublets. The intensity ratio between the two doublets reflects the natural abundance of the two silver isotopes (both isotopes ^{107}Ag and ^{109}Ag have a nuclear spin $I = 1/2$ and have a natural abundance of 52% and 48%, respectively) [14d]. As expected, the analogous copper complexes show no coupling pattern under similar conditions. The additional signal broadening for the phosphine copper(I) species (up to 9000 Hz) results from the quadrupole effect of the copper isotopes ^{63}Cu and ^{65}Cu ($I = 3/2$), respectively, which makes the appropriate studies in comparison to silver more complicated [15].

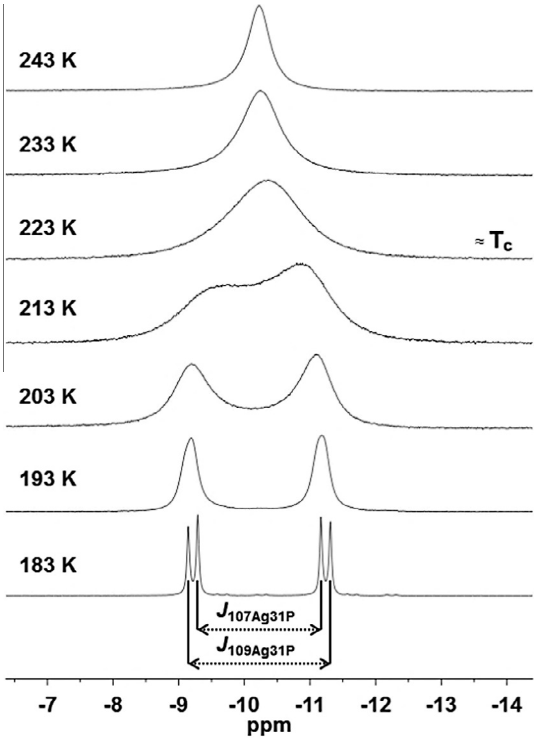

Fig. 2. Temperature-dependent $^{31}P\{^1H\}$ NMR spectra of **8a** in D$_2$-dichloromethane (temperature range: 183–243 K).

The temperature dependent $^{31}P\{^1H\}$ NMR spectra of representative [Ag(PBu$_3$)$_2$(S$_2$CNMe(C$_2$H$_4$OH))] (**8a**) are shown in Fig. 2.

The broad singlet observed for **8a** at −9.6 ppm (298 K, not depicted) in the $^{31}P\{^1H\}$ NMR spectra starts broadening by lowering the temperature resulting in a broad doublet between 223 and 213 K (coalescence temperature, T_c), which sharpens until 193 K (Fig. 2). It is well known that in NMR spectroscopy variable temperature lead to a shift of the resonance signals [14a,16]. This phenomenon is also found for [Ag(PBu$_3$)$_2$(S$_2$CNMe(C$_2$H$_4$OH))] (**8a**) (298 K, −9.6 ppm; 183 K, −10.2 ppm). At 183 K the signals are sharp enough to allow the extraction of the two coupling constants $J_{^{107}Ag^{31}P} = 380$ Hz and $J_{^{109}Ag^{31}P} = 440$ Hz (Fig. 2). This finding is also in agreement with phosphine silver(I) carboxylates of general type [AgL$_n$(O$_2$CR)]/[AgL$_4$][O$_2$CR] (L = phosphine, phosphite; n = 1, 2, 3; R = single bonded organic group) [14], *i.e.* [Ag(PBu$_3$)$_n$(O$_2$CMe)]/[Ag(PBu$_3$)$_4$][O$_2$CMe] [14a].

To further investigate complex [Ag(PBu$_3$)$_n$(S$_2$CNMe(C$_2$H$_4$OH))], the influence of the number n (n = 1.0, 1.5, 2.0, 2.5, 3.0, 3.5, 4.0, 4.5) of the PBu$_3$ ligands was investigated by $^{31}P\{^1H\}$ NMR spectroscopy at 183 K (Fig. 3, *top*). Subsequent addition of free phosphine PBu$_3$ ($\delta = -32.3$ ppm) [17] to [Ag(S$_2$CNMe(C$_2$H$_4$OH))] resulted in well-resolved and separated signals for three distinct species ([Ag(PBu$_3$)(S$_2$CNMe(C$_2$H$_4$OH))] (**7**): −3.9 ppm; [Ag(PBu$_3$)$_2$(S$_2$CNMe(C$_2$H$_4$OH))] (**8a**): −10.2 ppm; [Ag(PBu$_3$)$_4$][(S$_2$CNMe(C$_2$H$_4$OH))]: −19.2 ppm) (Fig. 3, Section 4). While in **7** the phosphine ligand gives rise to a signal at −3.9 ppm in the $^{31}P\{^1H\}$ NMR spectrum, the further coordination of a PBu$_3$ ligand to silver led to a resonance signal at higher field. This is in accordance with the concept that the Lewis acidity of silver(I) decreases resulting in a less deshielding of the phosphors atom. Furthermore, J_{AgP} were largest in the *mono*-phosphine silver(I) complex **7** ($J_{^{107}Ag^{31}P} = 549$ Hz, $J_{^{109}Ag^{31}P} = 634$ Hz) and becomes smallest in the *tetrakis*(phosphine) species [Ag(PBu$_3$)$_4$][(S$_2$CNMe(C$_2$H$_4$OH))] ($J_{^{107}Ag^{31}P} = 219$ Hz, $J_{^{109}Ag^{31}P} = 252$ Hz) via **8a** ($J_{^{107}Ag^{31}P} = 380$ Hz, $J_{^{109}Ag^{31}P} = 440$ Hz) (Fig. 3, *top*), which can be explained by the weakening of the Ag–P bond with increasing numbers of PBu$_3$ at silver and a lower 5s(Ag) character of the Ag–P bond. The trend in the coupling constants is very similar to the silver(I) carboxylate system of type [Ag(PBu$_3$)$_n$(O$_2$CMe)]/[Ag(PBu$_3$)$_4$][O$_2$CMe] previously reported [14a].

In contrast to similar carboxylate systems [14], [AgL$_3$(S$_2$CNMe(C$_2$H$_4$OH))] was not observed. This is best seen for the spectra with $n \approx 3$ (Fig. 3, *top*), where two species are visible. The first species (−10.3 ppm) can be assigned to [AgL$_2$(S$_2$CNMe(C$_2$H$_4$OH))] as it appears as the only system in the spectra with $n \approx 2$. The second (−19.2 ppm) is [AgL$_4$][S$_2$CNMe(C$_2$H$_4$OH)], which is an accordance to other [AgL$_4$]$^+$ coordination complexes, *i.e.* [Ag(PBu$_3$)$_4$][O$_2$CMe] [14a]. Obviously the dithiocarbamate ligand strongly prefers a κ^2-S,S′ coordination mode [1], as found in the solid state structure for the PPh$_3$ analogue **12a** (vide infra, X-ray structure and [18]). Therefore, the expected complex [AgL$_3$(S$_2$CNMe(C$_2$H$_4$OH))], which requires a monodentate binding mode of the dithiocarbamate, is destabilized and hence not observed.

The *bis*(phosphine) adduct [AgL$_2$(S$_2$CNMe(C$_2$H$_4$OH))] is the preferred species within this system. This can be concluded from the spectra with n ≈ 2, since only very small (less than 5%) additional signals ([AgL(S$_2$CNMe(C$_2$H$_4$OH))], −3.9 ppm; [AgL$_4$][S$_2$CNMe(C$_2$H$_4$OH)], −19.2 ppm) to the main species [AgL$_2$(S$_2$CNMe(C$_2$H$_4$OH))] appear. Clearly, this distribution of [AgL$_n$(S$_2$CNMe(C$_2$H$_4$OH))]/[AgL$_4$][S$_2$CNMe(C$_2$H$_4$OH)] (n = 1, 2) does not reflect the statistical distribution. This shows that a disproportionation of three equivalents

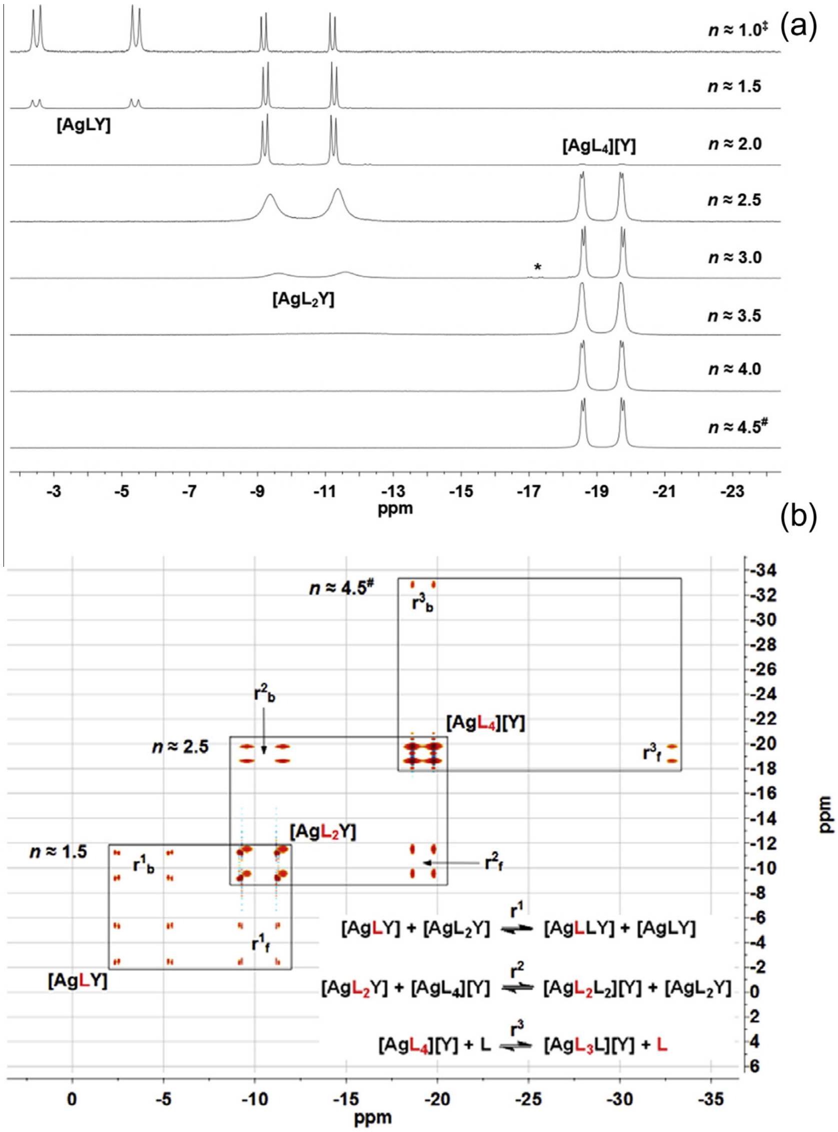

Fig. 3. a) $^{31}P\{^{1}H\}$ NMR spectra of complexes resulting from $[AgS_2CNMe(C_2H_4OH)]$ (**11a**) and *n* equivalents of PBu_3 ($n \approx 1.0, 1.5, 2.0, 2.5, 3.0, 3.5, 4.0, 4.5$) in D_2-dichloromethane at 183 K. (*free $PBu_2{}^{sec}Bu$, always present as trace in PBu_3. Please, notice that this may have an influence on the line widths and the signal positions; ‡for $n \approx 1$ some precipitation afforded **11a** along with higher concentration of $[AgL_2S_2CNMe(C_2H_4OH)]$; #for $n \approx 4.5$ a broad signal of free L at −32 ppm arises). b) Combination of three $^{31}P\{^{1}H\}$ EXSY NMR spectra of $[Ag(PBu_3)_nS_2CNMe(C_2H_4OH)]$ ($n \approx 1.5, 2.5, 4.5$) in D_2-dichloromethane at 183 K (0.4, 0.2, 0.4 s mixing time, respectively). (Cross peaks have been assigned to the three reaction r^1, r^2 and r^3, the lower indices give the reaction direction (f = forward, b = backward). (#for $n \approx 4.5$ additional signals of free L arise at −32 ppm.).

$[AgL_2(S_2CNMe(C_2H_4OH))]$ to two $[AgL(S_2CNMe(C_2H_4OH))]$ and one $[AgL_4][S_2CNMe(C_2H_4OH)]$ is disfavored. In spectra with $n > 4$ a broad singlet corresponding to free PBu_3 was observed.

In order to gain a deeper insight into the exchange mechanism of the phosphines, $^{31}P\{^{1}H\}$ EXSY NMR spectra were recorded (Fig. 3, *bottom*). These spectra show the expected cross peaks for a stepwise phosphine exchange.

To further prove the identity and phosphine silver ratio *n* especially for $[AgL_2(S_2CNMe(C_2H_4OH)]$ a mixed complex $[AgLL'(S_2CNMe(C_2H_4OH)]$ was prepared by adding one equivalent of P^cHex_3 (L′) to a solution of $[Ag(PBu_3)(S_2CNMe(C_2H_4OH))]$ (**7**) in D_2-dichloromethane as depicted in Eq. (1). The formation of $[AgLL'(S_2CNMe(C_2H_4OH)]$ was monitored by $^{31}P\{^{1}H\}$, $^{31}P,^{31}P\{^{1}H\}$ COSY and $^{31}P\{^{1}H\}$ EXSY NMR spectroscopy (Fig. 4). The $^{31}P\{^{1}H\}$ NMR spectrum reveals the presence of a 2:0.3:0.6 mixture of $[AgLL'(S_2CNMe(C_2H_4OH)]$, $[AgL'_2(S_2CNMe(C_2H_4OH)]$ and $[AgL_2(S_2CNMe(C_2H_4OH)]$, respectively (Eq. (1)). The $^{31}P\{^{1}H\}$ NMR signals corresponding to L′ are located at ca. 25 ppm, while signals for L (PBu_3) were found around −12 ppm (Fig. 4, *top*). As discussed above, the more electron-donating ligand P^cHex_3 let arise the new signal at higher field. Nevertheless, the coupling constants $J_{^{107}Ag^{31}P}$ (360–400 Hz) and $J_{^{109}Ag^{31}P}$ (420–460 Hz) fall in the typical range of *bis*(phosphine) adducts [14a,17] (vide supra). The two signals assigned to $[AgLL'(S_2CNMe(C_2H_4OH)]$ allow extraction of the phosphorous–phosphorous coupling constant ($^{2}J_{PP} = 110$ Hz), and the coupling pattern agrees to a 1:1 ratio between L and L′ in $[AgLL'(S_2CNMe(C_2H_4OH)]$. The coupling pathways are further illustrated by the $^{31}P–^{31}P\{^{1}H\}$ COSY NMR spectrum shown in Fig. 4

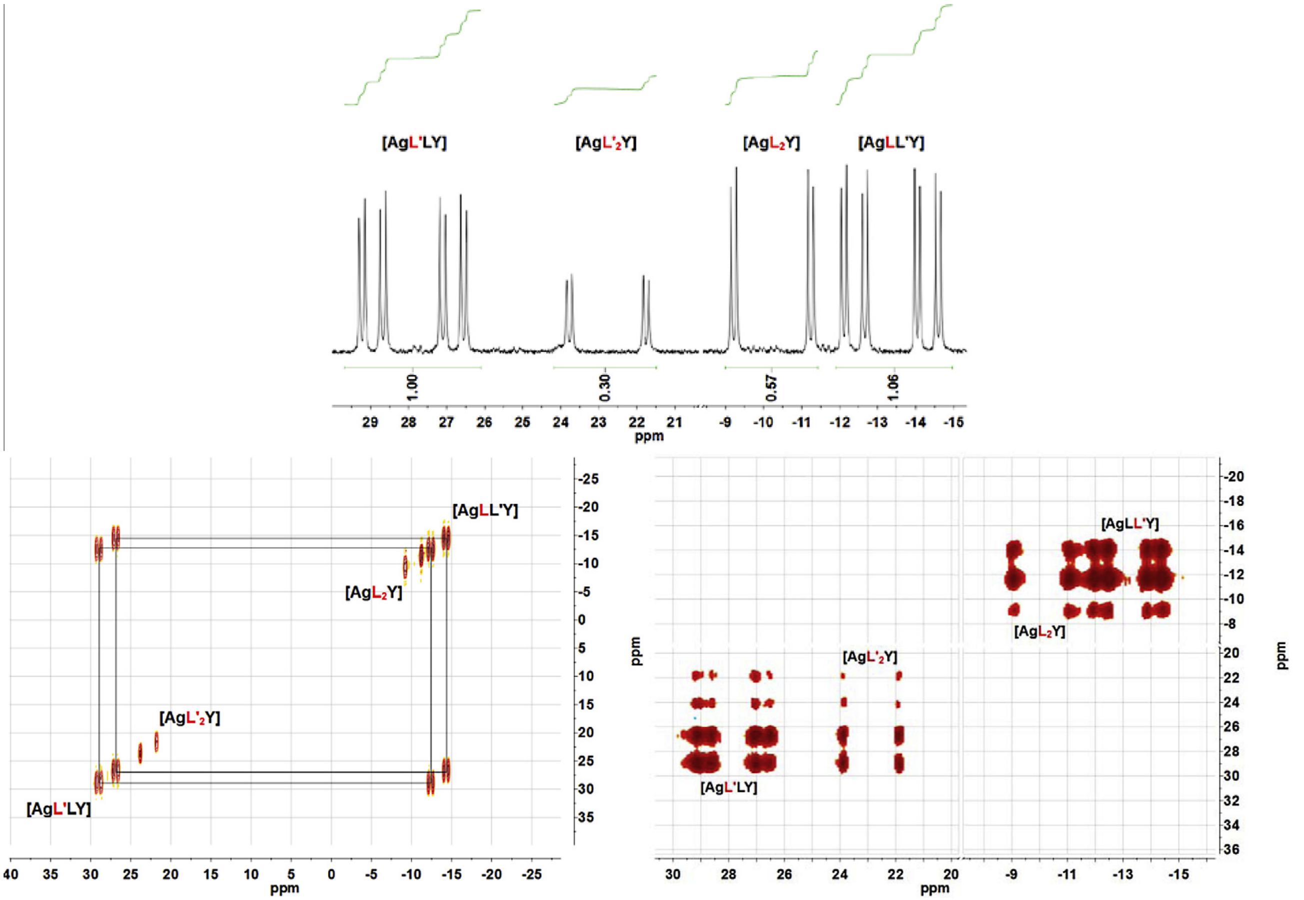

Fig. 4. *Top*: $^{31}P\{^{1}H\}$ NMR spectra of complexes resulting from [Ag(PBu$_3$)(S$_2$CNMe(C$_2$H$_4$OH))] (**7**) and one equivalent of P^{c}Hex$_3$ in D$_2$-dichloromethane at 183 K. *Bottom, left*: ^{31}P–$^{31}P\{^{1}H\}$ COSY NMR spectrum of **7** and P^{c}Hex$_3$ in D$_2$-dichloromethane at 183 K. *Bottom, right*: ^{31}P–$^{31}P\{^{1}H\}$ EXSY NMR spectrum of **7** and P^{c}Hex$_3$ in D$_2$-dichloromethane at 213 K (0.2 s mixing time).

(*bottom left*). The ^{31}P–$^{31}P\{^{1}H\}$ EXSY NMR spectrum presents the expected cross peaks proving phosphine exchange between all three species. In summary, this allows undoubtedly the determination of the silver ligand ratios *n* in the system [AgL$_n$(S$_2$CNMe(C$_2$H$_4$OH)]/[AgL$_4$][S$_2$CNMe(C$_2$H$_4$OH)] ($n = 1, 2$).

$$[\mathrm{AgLY}] \xrightarrow{\mathrm{L'}} [\mathrm{AgLL'Y}] \rightleftharpoons 0.5\,[\mathrm{AgL_2Y}] + 0.5\,[\mathrm{AgL'_2Y}] \qquad (1)$$

7 **7** + L' **8a**

L = PBu$_3$, L' = P^{c}Hex$_3$, Y = S$_2$CNMe(C$_2$H$_4$OH)

The molecular structures of [Ag(PPh$_3$)$_2$(S$_2$CNMe(C$_2$H$_4$OH))] (**12a**) and [Ag(PPh$_3$)$_2$(S$_2$CNBu(C$_2$H$_4$OH))] (**12b**) in the solid state were established by single X-ray structure analysis. Single crystals could be grown from slow diffusion of diethyl ether into a saturated solution containing **12a** or **12b** in dichloromethane at ambient temperature. Complexes **12a**,**b** crystallize in the triclinic space group $P\bar{1}$. The bond lengths of both complexes differ up to 3% and corresponding bond angles up to 8%. Selected bond distances (Å) and angles (°) are summarized in Table 2. For important crystal data, collection and refinement parameters see Section 4. The molecular structures of **12a**,**b** are illustrated in Fig. 5.

Both complexes are monomeric revealing a chelating κ^2-S,S′ binding mode of the dithiocarbamate ligand, which is by far the most common structural motif. [1] The Ag(I) ion possesses a somewhat distorted tetrahedral AgP$_2$S$_2$ coordination environment, setup by two datively-bonded PPh$_3$ ligands and one chelated dithiocarbamate group (Fig. 5). The bond distances and bond angles of **12a**,**b** correlate with those values found for similar complexes, *i.e.* [Ag(PPh$_3$)$_2$(S$_2$CN(CH$_2$)$_4$))] [18].

Table 2
Selected bond distances [Å] and angles [°] for **12a**,**b** [a].

12a		**12b**	
Bond distances			
Ag1–S1	2.6592(9)	Ag1–S1	2.6090(10)
Ag1–S2	2.6380(9)	Ag1–S2	2.6717(10)
Ag1–P1	2.4964(9)	Ag1–P1	2.4255(10)
Ag1–P2	2.4172(8)	Ag1–P2	2.4658(10)
C1–S1	1.720(4)	C1–S1	1.714(4)
C1–S2	1.732(4)	C1–S2	1.727(4)
C1–N1	1.333(5)	C1–N1	1.341(5)
Bond angles			
P1–Ag1–P2	122.53(3)	P1–Ag1–P2	123.52(3)
P1–Ag1–S1	95.01(3)	P1–Ag1–S1	125.31(3)
P1–Ag1–S2	108.10(3)	P1–Ag1–S2	114.54(3)
P2–Ag1–S1	131.93(3)	P2–Ag1–S1	103.12(3)
P2–Ag1–S2	118.11(3)	P2–Ag1–S2	108.66(3)
S1–Ag1–S2	68.35(3)	S1–Ag1–S2	68.48(3)
Ag1–S1–C1	83.29(13)	Ag1–S1–C1	85.74(15)
Ag1–S2–C1	84.16(12)	Ag1–S2–C1	83.54(14)
S1–C1–S2	119.1(2)	S1–C1–S2	119.4(2)
N1–C1–S1	120.3(3)	N1–C1–S1	120.3(3)
N1–C1–S2	120.6(3)	N1–C1–S2	120.2(3)

[a] The estimated standard deviation(s) of the last significant digits are shown in parentheses.

TG (=Thermogravimetry) studies of selected samples were carried out to gain first information on the thermal behavior of the respective dithiocarbamate copper(I) and silver(I) complexes in

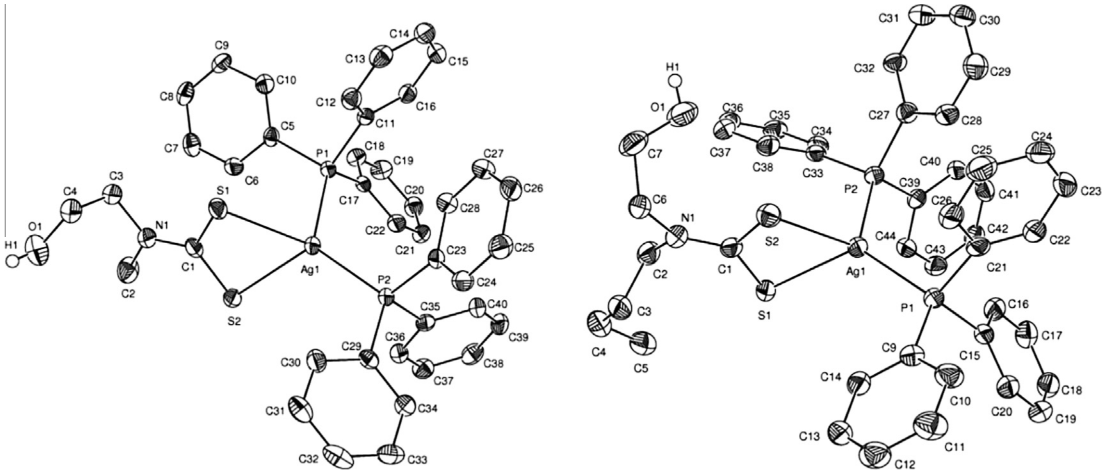

Fig. 5. ORTEP diagrams (50% probability level) of **12a** (left) and **12b** (right). For disordered atoms only one set is shown. All hydrogen atoms, except for the *O*-bonded hydrogen atoms, are omitted for clarity.

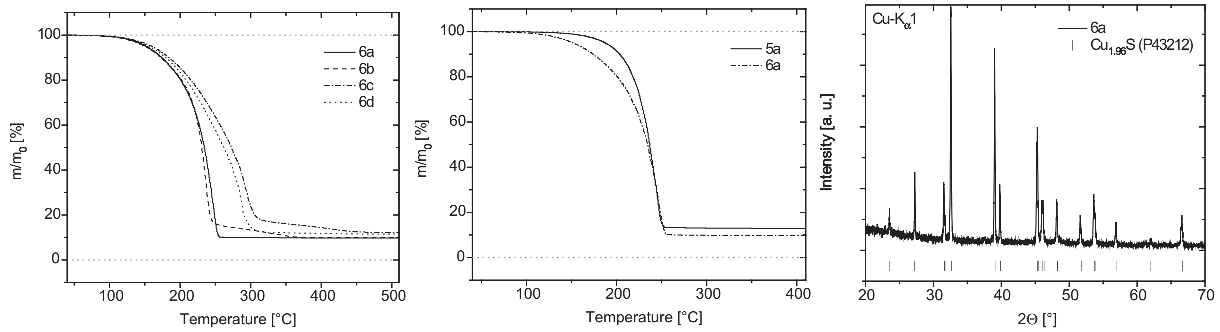

Fig. 6. *Left*: TG traces (N_2, flow rate 60 mL min^{-1}, heating rate 10 K min^{-1}) of **6a**–**d**. *Middle*: TG traces (N_2, flow rate 60 mL min^{-1}, heating rate 10 K min^{-1}) of **5a** and **6a**. *Right*: XRPD pattern of the TG residue of **6d** showing peaks for $Cu_{1.96}S$ [tetr. chalcocite, JCPDS 29-0578].

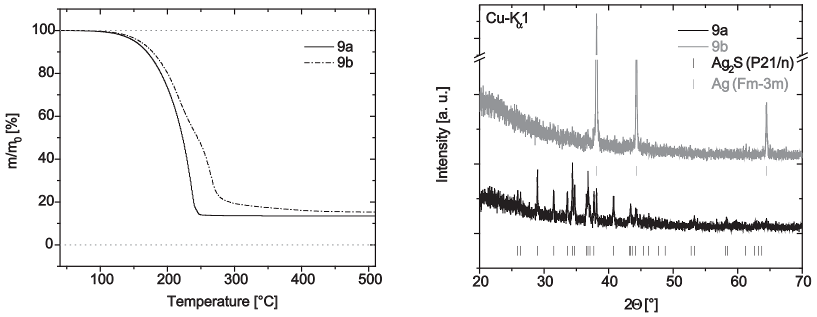

Fig. 7. *Left*: TG traces (N_2, flow rate 60 mL min^{-1}, heating rate 10 K min^{-1}) of **9a** and **9b**. *Right*: XRPD pattern of the TG residue of **9a** and **9b** showing peaks for Ag [JCPDS 04-0783] and α-Ag_2S [acanthite, JCPDS 14-0072].

the solid state. The appropriate TG traces are shown in Figs. 6 and 7. These Figures also include the XRPD pattern of the TG residues obtained. The studies were conducted at atmospheric pressure under a nitrogen purge (60 mL min^{-1}) with a constant heating rate of 10 K min^{-1}. Thermal decomposition characteristics are summarized in Table 3.

From Fig. 6 it can be seen that the decomposition of complexes **6a**–**d** starts at ca. 75 °C and is completed depending on the nature of the dithiocarbamate ligand between 270 and 480 °C, whereby **6a**,**b** show with 210 °C the lowest onset temperatures, when compared with **6c**,**d** (ca. 250 °C). Fig. 6 also shows that complexes **6a**–**d** decompose in a one-step (**6a**) or two-step (**6b**–**d**) process with mass losses between 88.0 and 90.3% (Table 3). The difference between the observed and the calculated values for **6c**,**d** are with 2.5 and 1.5% higher than those ones for **6a**,**b**, correlating well with theoretical percentages calculated for Cu_2S. The higher deviation for **6c**,**d** is most probably attributed to carbon impurities. The respective TG residues were analyzed by XRPD studies (**6a**: Fig. 6, right). In these studies it was found that only the residues obtained from **6a**,**b** show crystalline Cu_xS (**6a**,**b**: tetr. chalcocite

Table 3
Thermal decomposition characteristics of **5**, **6**, and **9**.

	ϑ_i–ϑ_f [°C] (Δm [%])	ϑ_o [°C]	m/m_0 [%]	ω_{M2S} [%]	ω_M [%]	$m/m_0 - \omega_{M2S}$ [%]	XRPD[a]
5a	90–290 (87.2)	216	12.8	12.9		−0.1	$Cu_{1.96}S$
5b	90–300 (87.2)	221	12.8	12.3		0.5	$Cu_{1.96}S$
5c	90–600 (85.9)	255	14.1	12.5		1.6	-[b]
6a	70–270 (90.3)	210	9.7	9.7		0.0	$Cu_{1.96}S$
6b	75–380 (90.2)	211	9.8	9.4		0.4	Cu_2S, $Cu_{1.96}S$
6c	75–480 (88.0)	240	12.0	9.5		2.5	-[b]
6d	75–450 (88.7)	247	11.3	9.8		1.5	-[b]
9a	55–270 (86.6)	197	13.4	14.3	12.9	−0.9	Ag_2S/Ag
9b	60–520 (84.9)	232	15.1	14.0	12.2	1.1	Ag

ϑ_i: Initial decomposition temperature. ϑ_f: Final decomposition temperature. ϑ_o: Onset temperature. ω: Mass fraction. ω_{M2S}: Metal sulfide content, calcd. residue for solely formation of M_2S. ω_M: Metal content, calcd. residue for solely formation of M.

[a] Crystalline parts of TG residue analyzed by XRPD.

[b] No crystalline properties.

with $x = 1.96$; **6b**: β-chalcocite with $x = 2$). This discrepancy between **6a**,**b** and **6c**,**d** from the TG as well as the XRPD experiments can likely be explained by the proposed decomposition mechanism of (β-hydroxyethyl)-methyldithiocarbamates as recently published by Nomura et al. [19] and our group [20] (Scheme 2). The influence of the number n of the PBu_3 ligands present in the complex on the thermal induced decomposition is shown in Fig. 6 (*middle*). It was found that the higher the number n, the lower the initial decomposition temperature is, which is an accordance to other phosphine metal(I) carboxylate complexes [21].

The thermal behavior of phosphine silver(I) dithiocarbamates **9a**,**b** is compared in Fig. 7 (*left*) and shows initial temperatures of around 60 °C. While the one-step decomposition of **9a** is finished at ca. 270 °C, allyl-functionalized **9b** undergoes a multi-step decomposition, which is completed at ca. 500 °C. Both compounds reveal a discrepancy between found TG residue values (**9a**, 13.4%; **9b**, 15.1%) and the residue calculated for the solely formation of Ag_2S (**9a**, 14.3%; **9b**, 14.0%) (Table 3). Interestingly, in case of **9b** XRPD measurements of the respective TG residues (Fig. 7, right) display solely silver as crystalline material, while for **9a** majorly crystalline α-Ag_2S (acanthite) along with traces of silver is found. The in Scheme 2 proposed decomposition mechanism of (β-hydroxyethyl)-methyldithiocarbamates might be responsible for these findings.

3. Conclusion

Straightforward synthetic methodologies for the preparation of a series of phosphine dithiocarbamate copper(I) and silver(I) complexes of type $[M(PBu_3)_n(S_2CNRR')]$ (M = Cu, Ag; $n = 1, 2, 3$; $R = R' = CH_2CH{=}CH_2$, $(CH_2)_4$, C_2H_4OH; R = Me, $R' = C_2H_4OH$; R = Bu, $R' = C_2H_4OH$) are described. $^{31}P\{^1H\}$ NMR studies of $[Ag(PBu_3)_n(S_2CNMe(C_2H_4OH)]$ ($n = 1.0, 1.5, 2.0, 2.5, 3.0, 3.5, 4.0, 4.5$) and $[Ag(PBu_3)(P^cHex_3)(S_2CNMe(C_2H_4OH))]$ in the temperature range of 308–178 K prove phosphine ligand exchange processes in solution. 2D NMR Experiments allowed the determination of the silver ligand ratios n in the system $[AgL_n(S_2CNMe(C_2H_4OH)]/[AgL_4][S_2CNMe(C_2H_4OH)]$ ($n = 1, 2$) and reveal the *bis*(phosphine) adduct $[AgL_2(S_2CNMe(C_2H_4OH))]$ as preferred species. Single X-ray structure analysis verify the monomeric structures of $[Ag(PPh_3)_2(S_2CNR(C_2H_4OH))]$ (R = Me, Bu) in the solid state. Dithiocarbamate $S_2CNR(C_2H_4OH)$ is thereby chelate-bonded κ^2-S,S′ to the silver atom. Thermogravimetric studies were carried out for selected samples. By varying the substituents at the dithiocarbamate nitrogen atom a decreasing of the onset temperatures for the decomposition was achieved. The respective decomposition residues (Cu_xS, $x = 1.96, 2$; Ag, Ag_2S) were characterized by XRPD. Due to their thermal properties, especially complexes $[M(PBu_3)_2(S_2CNMe(C_2H_4OH)]$ (M = Cu, Ag) are excellent candidates for the deposition of copper- and silver-sulfides using different deposition techniques including CVD (=Chemical Vapor Deposition) and spin-coating processes. This single source precursor (=SSP) approach allows the formation of thin layers for potential applications in solar selective coatings and IR detectors which can be generated much more safe then common methods using hazardous sulfur sources.

4. Experimental

4.1. General

All reactions were carried out under an argon or nitrogen atmosphere using standard Schlenk techniques. Hexane and pentane were purified by distillation from sodium/benzophenone ketyl; acetonitrile and dichloromethane from calcium hydride and ethanol from sodium and diethylphthalate. The NMR solvents were dried over molecular sieve and were stored under argon atmosphere.

4.2. Instruments

FT-IR spectra were recorded with a Thermo Nicolet IR 200 spectrometer. NMR spectra were recorded with a Bruker Avance III 500 spectrometer (500.3 MHz for ^1H, 125.7 MHz for $^{13}C\{^1H\}$ and 202.5 MHz for $^{31}P\{^1H\}$). Chemical shifts are reported in δ (parts per million) units downfield from tetramethylsilane ($\delta = 0.0$) with the solvent as reference signal (^1H NMR: $CDCl_3$, $\delta = 7.26$; CD_2Cl_2, $\delta = 5.32$; CD_3OD, $\delta = 3.31$, DMSO-d_6, $\delta = 2.50$. $^{13}C\{^1H\}$ NMR: $CDCl_3$, $\delta = 77.16$; CD_2Cl_2, $\delta = 54.00$; CD_3OD, $\delta = 49.00$; DMSO-d_6, $\delta = 39.52$. $^{31}P\{^1H\}$ NMR: standard external rel. 85% H_3PO_4, $\delta = 0.0$; $P(OMe)_3$, $\delta = 139.0$.). $^{31}P\{^1H\}$ NMR spectra were recorded under conditions of broad band proton decoupling in $CDCl_3$ or CD_2Cl_2. For low temperature experiments CD_2Cl_2 solutions (0.6 mL) of the respective complex (0.1 mmol) were prepared. Temperatures were varied by passing either pre-cooled or pre-heated dry nitrogen over the sample, and 5 min were allowed for equilibration.

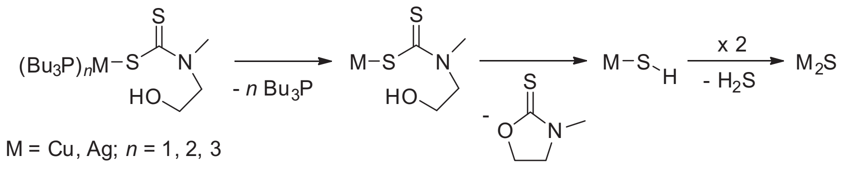

Scheme 2. Proposed decomposition mechanism of (β-hydroxyethyl)-methyl-functionalized dithiocarbamates.

The melting points were determined using a Gallenkamp MFB 595 010 M melting point apparatus. Microanalyses were performed with a *C*, *H*, *N* analyzer FlashAE 1112 instrument (Thermo Company). TG experiments were performed with a Mettler Toledo TGA/DSC1 1100 system with an UMX1 balance. Powder X-ray diffraction patterns of all samples were obtained with a STOE-STADI-P diffractometer using Cu Kα radiation (40 kV, 40 mA) and a Ge(111)-monochromator.

4.3. Reagents

Complexes $[\mathrm{Cu(PBu_3)}_n\mathrm{Cl}]$ and $[\mathrm{Ag(PBu_3)}_n\mathrm{(NO_3)}]$ [22] (n = 1, 2, 3), $\mathrm{K[S_2CNRR']}$ [9,20] ($\mathrm{R = R' = CH_2CH{=}CH_2}$, $\mathrm{(CH_2)_4}$, $\mathrm{C_2H_4OH}$; R = Me, $\mathrm{R' = C_2H_4OH}$; R = Bu, $\mathrm{R' = C_2H_4OH}$), $[\mathrm{Ag(S_2CN(CH_2CH{=}CH_2)_2)}]$, [23] $[\mathrm{Ag(S_2CNMe(C_2H_4OH))}]$ and $[\mathrm{Ag(S_2CNBu(C_2H_4OH))}]$ [20] were prepared by published procedures. All other chemicals were purchased by commercial suppliers and were used as received.

4.3.1. Synthesis of $[K(S_2CNBu(C_2H_4OH))]$ (3e)

According to reference [9], **3e** was prepared as follows: Amine $\mathrm{NHBu(C_2H_4OH)}$ (12.30 g, 105 mmol) was added to an ethanolic solution (500 mL) of KOH (5.60 g, 100 mmol) at 0 °C. Afterwards, an ethanolic solution (100 mL) of $\mathrm{CS_2}$ (6.0 mL, 15.3 g, 200 mmol) was added dropwise. After stirring for 5 h at ambient temperature, the reaction mixture was concentrated under reduced pressure and dry diethyl ether was added until precipitation reached completion. Subsequently, **3e** was filtered, washed with diethyl ether (3 × 50 mL) and dried in *oil pump* vacuum. Compound **3e** was obtained as a colorless solid, soluble in ethanol and methanol. Yield: 21.97 g (95 mmol, 95% based on $\mathrm{NHBu(C_2H_4OH)}$). **Mp** 124 °C. *Anal.* Calc. for $\mathrm{C_7H_{14}KNOS_2}$ (231.42): C, 36.33; H, 6.10; N, 6.05. Found: C, 36.00; H, 6.07; N, 5.93%. **IR** (KBr): 3325 (O–H); 2943, 2924, 2864 (C–H); 1458 (C–N); 1108 (C–S) $\mathrm{cm^{-1}}$. **^{1}H NMR** ($\mathrm{CD_3OD}$): 4.79 (s, $\mathrm{O}\mathit{H}$, 1H), 4.22 (t, $^3J_{\mathrm{HH}}$ = 6 Hz, $\mathrm{NC}\mathit{H}_2\mathrm{CH_2OH}$, 2H), 4.14–4.08 (m, $\mathrm{NC}\mathit{H}_2\mathrm{(CH_2)_2CH_3}$, 2H), 3.89 (t, $^3J_{\mathrm{HH}}$ = 6 Hz, $\mathrm{NCH_2C}\mathit{H}_2\mathrm{OH}$, 2H), 1.77–1.71 (m, $\mathrm{NCH_2C}\mathit{H}_2\mathrm{CH_2CH_3}$, 2H), 1.38–1.30 (m, $\mathrm{N(CH_2)_2C}\mathit{H}_2\mathrm{CH_3}$, 2H), 0.95 (t, $^3J_{\mathrm{HH}}$ = 7 Hz, $\mathrm{N(CH_2)_3C}\mathit{H}_3$, 3H). **^{13}C{^{1}H} NMR** ($\mathrm{CD_3OD}$): 213.6 (s, $\mathrm{S_2}\mathit{C}\mathrm{N}$), 61.2 (s, $\mathrm{NCH_2}\mathit{C}\mathrm{H_2OH}$), 56.5/56.2 (s/s, $\mathrm{N}\mathit{C}\mathrm{H_2CH_2OH/N}\mathit{C}\mathrm{H_2(CH_2)_2CH_3}$), 30.0 (s, $\mathrm{NCH_2}\mathit{C}\mathrm{H_2CH_2CH_3}$), 21.1 (s, $\mathrm{N(CH_2)_2}\mathit{C}\mathrm{H_2CH_3}$), 14.3 (s, $\mathrm{N(CH_2)_3}\mathit{C}\mathrm{H_3}$). **HRMS** (ESI-TOF, neg. mode) $\mathrm{[M{-}K]^-}$, *m*/*z* Calcd.: 192.0511, Found: 192.0515.

4.3.2. Synthesis of Tri-n-butylphosphine copper(I) and silver(I) dithiocarbamates (4–9)

Complex $[\mathrm{Cu(PBu_3)}_n\mathrm{Cl}]$ (**1a**–**c**) (1.0 mmol) or $[\mathrm{Ag(PBu_3)}_n\mathrm{(NO_3)}]$ (**2a**–**c**) (1.0 mmol) was dissolved in pentane (50 mL) and $\mathrm{K[S_2CNRR']}$ (**3a**–**e**) (1.0 mmol) was added in a single portion at 0 °C. After stirring this suspension at ambient temperature for 10 h, filtration through a pad of Celite and evaporation of all volatiles in *oil-pump* vacuum gave the title complexes as pale yellow (Cu) or off-white (Ag) liquids.

4.3.2.1. $[Cu(PBu_3)(S_2CNMe(C_2H_4OH))]$ (***4***). Yield: 390 mg (0.93 mmol, 93% based on **1a**). *Anal.* Calc. for $\mathrm{C_{16}H_{35}CuNOPS_2}$ (416.10): C, 46.18; H, 8.48; N, 3.37. Found: C, 46.31; H, 8.55; N, 3.29%. **IR** (NaCl): 3388 (O–H); 2955, 2928, 2871 (C–H); 1463 (C–N); 1098 (C–S) $\mathrm{cm^{-1}}$. **^{1}H NMR** ($\mathrm{CDCl_3}$): δ 4.15 (t, $^3J_{\mathrm{H,H}}$ = 5 Hz, $\mathrm{NC}\mathit{H}_2\mathrm{CH_2OH}$, 2H), 3.88–3.85 (m, $\mathrm{NCH_2C}\mathit{H}_2\mathrm{OH}$, 2H), 3.41 (s, $\mathrm{NC}\mathit{H}_3$, 3H), 3.09 (t, $^3J_{\mathrm{H,H}}$ = 5 Hz, $\mathrm{O}\mathit{H}$, 1H), 1.58–1.34 (m, $\mathrm{PC}\mathit{H}_2\mathrm{C}\mathit{H}_2\mathrm{C}\mathit{H}_2\mathrm{CH_3}$, 18H), 0.89 (t, $^3J_{\mathrm{H,H}}$ = 7 Hz, $\mathrm{P(CH_2)_3C}\mathit{H}_3$, 9H). **^{13}C{^{1}H} NMR** ($\mathrm{CDCl_3}$): δ 211.0 (s, $\mathrm{S_2}\mathit{C}\mathrm{N}$), 61.8 (s, $\mathrm{N}\mathit{C}\mathrm{H_2CH_2OH}$), 56.3 (s, $\mathrm{NCH_2}\mathit{C}\mathrm{H_2OH}$), 41.3 (s, $\mathrm{N}\mathit{C}\mathrm{H_3}$), 26.5 (s, $\mathrm{P}\mathit{C}\mathrm{H_2(CH_2)_2CH_3}$), 25.4 (s, $\mathrm{PCH_2}\mathit{C}\mathrm{H_2CH_2CH_3}$), 24.8 (s, $\mathrm{P(CH_2)_2}\mathit{C}\mathrm{H_2CH_3}$), 13.9 (s, $\mathrm{P(CH_2)_3}\mathit{C}\mathrm{H_3}$). **^{31}P{^{1}H} NMR** ($\mathrm{CDCl_3}$): δ −16.9.

4.3.2.2. $[Cu(PBu_3)_2(S_2CNMe(C_2H_4OH))]$ (***5a***). Yield: 580 mg (0.94 mmol, 94% based on **1b**). *Anal.* Calc. for $\mathrm{C_{28}H_{62}CuNOP_2S_2}$ (618.42): C, 54.38; H, 10.11; N, 2.26. Found: C, 54.10; H, 10.03; N, 2.20% **IR** (NaCl): 3398 (O–H); 2956, 2928, 2871 (C–H); 1464 (C–N); 1096 (C–S) $\mathrm{cm^{-1}}$. **^{1}H NMR** ($\mathrm{CDCl_3}$): δ 4.15 (t, $^3J_{\mathrm{H,H}}$ = 5 Hz, $\mathrm{NC}\mathit{H}_2\mathrm{CH_2OH}$, 2H), 3.88 (q, $^3J_{\mathrm{H,H}}$ = 5 Hz, $\mathrm{NCH_2C}\mathit{H}_2\mathrm{OH}$, 2H), 3.41 (s, $\mathrm{NC}\mathit{H}_3$, 3H), 3.09 (t, $^3J_{\mathrm{H,H}}$ = 5 Hz, $\mathrm{O}\mathit{H}$, 1H), 1.53–1.49 (m, $\mathrm{PC}\mathit{H}_2\mathrm{(CH_2)_2CH_3}$, 12H), 1.46–1.40 (m, $\mathrm{PCH_2C}\mathit{H}_2\mathrm{CH_2CH_3}$, 12H), 1.38–1.31 (m, $\mathrm{P(CH_2)_2C}\mathit{H}_2\mathrm{CH_3}$, 12H), 0.87 (t, $^3J_{\mathrm{H,H}}$ = 7 Hz, $\mathrm{P(CH_2)_3C}\mathit{H}_3$, 18H). **^{13}C{^{1}H} NMR** ($\mathrm{CDCl_3}$): δ 211.1 (s, $\mathrm{S_2}\mathit{C}\mathrm{N}$), 61.8 (s, $\mathrm{N}\mathit{C}\mathrm{H_2CH_2OH}$), 56.3 (s, $\mathrm{NCH_2}\mathit{C}\mathrm{H_2OH}$), 41.4 (s, $\mathrm{N}\mathit{C}\mathrm{H_3}$), 26.9 (s, $\mathrm{P}\mathit{C}\mathrm{H_2(CH_2)_2CH_3}$), 25.6 (s, $\mathrm{PCH_2}\mathit{C}\mathrm{H_2CH_2CH_3}$), 24.8 (s, $\mathrm{P(CH_2)_2}\mathit{C}\mathrm{H_2CH_3}$), 13.9 (s, $\mathrm{P(CH_2)_3}\mathit{C}\mathrm{H_3}$). **^{31}P{^{1}H} NMR** ($\mathrm{CDCl_3}$): δ −18.7.

4.3.2.3. $[Cu(PBu_3)_2(S_2CN(C_2H_4OH)_2)]$ (***5b***). Yield: 590 mg (0.91 mmol, 91% based on **1b**). *Anal.* Calc. for $\mathrm{C_{29}H_{64}CuNO_2P_2S_2}$ (648.45): C, 53.71; H, 9.95; N, 2.16. Found: C, 53.33; H, 9.88; N, 2.16%. **IR** (NaCl): 3406 (O–H); 2956, 2927, 2869 (C–H); 1463 (C–N); 1100 (C–S) $\mathrm{cm^{-1}}$. **^{1}H NMR** ($\mathrm{CDCl_3}$): δ 4.16 (t, $^3J_{\mathrm{H,H}}$ = 5 Hz, $\mathrm{NC}\mathit{H}_2\mathrm{CH_2OH}$, 4H), 3.95 (bs, $\mathrm{NCH_2C}\mathit{H}_2\mathrm{OH}$, 4H), 3.41 (s, $\mathrm{O}\mathit{H}$, 2H), 1.47–1.33 (m, $\mathrm{PC}\mathit{H}_2\mathrm{C}\mathit{H}_2\mathrm{C}\mathit{H}_2\mathrm{CH_3}$, 36H), 0.88 (t, $^3J_{\mathrm{H,H}}$ = 7 Hz, $\mathrm{P(CH_2)_3C}\mathit{H}_3$, 18H). **^{13}C{^{1}H} NMR** ($\mathrm{CDCl_3}$): δ 212.5 (s, $\mathrm{S_2}\mathit{C}\mathrm{N}$), 61.8 (s, $\mathrm{N}\mathit{C}\mathrm{H_2CH_2OH}$), 55.9 (s, $\mathrm{NCH_2}\mathit{C}\mathrm{H_2OH}$), 27.0 (s, $\mathrm{P}\mathit{C}\mathrm{H_2(CH_2)_2CH_3}$), 25.7 (s, $\mathrm{PCH_2}\mathit{C}\mathrm{H_2CH_2CH_3}$), 24.9 (s, $\mathrm{P(CH_2)_2}\mathit{C}\mathrm{H_2CH_3}$), 13.9 (s, $\mathrm{P(CH_2)_3}\mathit{C}\mathrm{H_3}$). **^{31}P{^{1}H} NMR** ($\mathrm{CDCl_3}$): δ −19.0.

4.3.2.4. $[Cu(PBu_3)_2(S_2CN(CH_2CH{=}CH_2)_2)]$ (***5c***). Yield: 560 mg (0.87 mmol, 87% based on **1b**). *Anal.* Calc. for $\mathrm{C_{31}H_{64}CuNP_2S_2}$ (640.47): C, 58.13; H, 10.07; N, 2.19. Found: C, 58.43; H, 9.99; N, 2.05%. **IR** (NaCl): 3390 (O–H); 2955, 2925, 2874 (C–H); 1463 (C–N); 1096 (C–S) $\mathrm{cm^{-1}}$. **^{1}H NMR** ($\mathrm{CDCl_3}$): δ 5.88–5.81 (m, $\mathrm{NCH_2C}\mathit{H}\mathrm{CH_2}$, 2H), 5.11 (ddd, $^3J_{\mathrm{H,H}}$ = 6 Hz, $^3J_{\mathrm{H,H}}$ = 6 Hz, $^3J_{\mathrm{H,H}}$ = 6 Hz, $\mathrm{NCH_2CHC}\mathit{H}_2$, 4H), 4.53 (d, $^3J_{\mathrm{H,H}}$ = 6 Hz, $\mathrm{NC}\mathit{H}_2\mathrm{CHCH_2}$, 4H), 1.50–1.40 (m, $\mathrm{P(C}\mathit{H}_2\mathrm{)_2CH_2CH_3}$, 36H), 1.38–1.31 (m, $\mathrm{P(CH_2)_2C}\mathit{H}_2\mathrm{CH_3}$, 18H), 0.87 (t, $^3J_{\mathrm{H,H}}$ = 7 Hz, $\mathrm{P(CH_2)_3C}\mathit{H}_3$, 27H). **^{13}C{^{1}H} NMR** ($\mathrm{CDCl_3}$): δ 210.7 (s, $\mathrm{S_2}\mathit{C}\mathrm{N}$), 133.0 (s, $\mathrm{NCH_2}\mathit{C}\mathrm{HCH_2}$), 116.9 (s, $\mathrm{NCH_2CH}\mathit{C}\mathrm{H_2}$), 53.4 (s, $\mathrm{N}\mathit{C}\mathrm{H_2CHCH_2}$), 27.0 (s, $\mathrm{P}\mathit{C}\mathrm{H_2(CH_2)_2CH_3}$), 25.7 (s, $\mathrm{PCH_2}\mathit{C}\mathrm{H_2CH_2CH_3}$), 24.9 (s, $\mathrm{P(CH_2)_2}\mathit{C}\mathrm{H_2CH_3}$), 14.0 (s, $\mathrm{P(CH_2)_3}\mathit{C}\mathrm{H_3}$). **^{31}P{^{1}H} NMR** ($\mathrm{CDCl_3}$): δ −18.5.

4.3.2.5. $[Cu(PBu_3)_3(S_2CNMe(C_2H_4OH))]$ (***6a***). Yield: 760 mg (0.93 mmol, 93% based on **1c**). *Anal.* Calc. for $\mathrm{C_{40}H_{89}CuNOP_3S_2}$ (820.74): C, 58.54; H, 10.93; N, 1.71. Found: C, 58.16; H, 10.95; N, 1.62%. **IR** (NaCl): 3369 (O–H); 2950, 2862 (C–H); 1462 (C–N); 1098 (C–S) $\mathrm{cm^{-1}}$. **^{1}H NMR** ($\mathrm{CDCl_3}$): δ 4.15 (t, $^3J_{\mathrm{H,H}}$ = 5 Hz, $\mathrm{NC}\mathit{H}_2\mathrm{CH_2OH}$, 2H), 3.89–3.86 (m, $\mathrm{NCH_2C}\mathit{H}_2\mathrm{OH}$, 2H), 3.41 (s, $\mathrm{NC}\mathit{H}_3$, 3H), 3.09 (t, $^3J_{\mathrm{H,H}}$ = 5 Hz, $\mathrm{O}\mathit{H}$, 1H), 1.46–1.32 (m, $\mathrm{P(C}\mathit{H}_2\mathrm{)_3CH_3}$, 54H), 0.87 (t, $^3J_{\mathrm{H,H}}$ = 7 Hz, $\mathrm{P(CH_2)_3C}\mathit{H}_3$, 27H). **^{13}C{^{1}H} NMR** ($\mathrm{CDCl_3}$): δ 211.2 (s, $\mathrm{S_2}\mathit{C}\mathrm{N}$), 61.8 (s, $\mathrm{N}\mathit{C}\mathrm{H_2CH_2OH}$), 56.2 (s, $\mathrm{NCH_2}\mathit{C}\mathrm{H_2OH}$), 41.3 (s, $\mathrm{N}\mathit{C}\mathrm{H_3}$), 27.3 (s, $\mathrm{P}\mathit{C}\mathrm{H_2(CH_2)_2CH_3}$), 26.1 (s, $\mathrm{PCH_2}\mathit{C}\mathrm{H_2CH_2CH_3}$), 24.8 (d, $^3J_{\mathrm{C,P}}$ = 10 Hz, $\mathrm{P(CH_2)_2}\mathit{C}\mathrm{H_2CH_3}$), 13.9 (s, $\mathrm{P(CH_2)_3}\mathit{C}\mathrm{H_3}$). **^{31}P{^{1}H} NMR** ($\mathrm{CDCl_3}$): δ −20.8.

4.3.2.6. $[Cu(PBu_3)_3(S_2CN(C_2H_4OH)_2)]$ (***6b***). Yield: 765 mg (0.90 mmol, 90% based on **1c**). *Anal.* Calc. for $\mathrm{C_{41}H_{91}CuNO_2P_3S_2}$ (850.76): C, 57.88; H, 10.78; N, 1.65. Found: C, 57.66; H, 10.60; N, 1.53%. **IR** (NaCl): 3393 (O–H); 2950, 2924, 2870 (C–H); 1468 (C–N); 1098 (C–S) $\mathrm{cm^{-1}}$. **^{1}H NMR** ($\mathrm{CDCl_3}$): δ 4.16 (t, $^3J_{\mathrm{H,H}}$ = 5 Hz, $\mathrm{NC}\mathit{H}_2\mathrm{CH_2OH}$, 4H), 3.95 (bs, $\mathrm{NCH_2C}\mathit{H}_2\mathrm{OH}$, 4H), 3.41 (s, $\mathrm{O}\mathit{H}$, 2H), 1.47–1.33 (m, $\mathrm{P(C}\mathit{H}_2\mathrm{)_3CH_3}$, 54H), 0.88 (t, $^3J_{\mathrm{H,H}}$ = 7 Hz, $\mathrm{P(CH_2)_3C}\mathit{H}_3$, 27H). **^{13}C{^{1}H} NMR** ($\mathrm{CDCl_3}$): δ 212.5 (s, $\mathrm{S_2}\mathit{C}\mathrm{N}$), 61.3 (s, $\mathrm{N}\mathit{C}\mathrm{H_2CH_2OH}$), 55.9 (s, $\mathrm{NCH_2}\mathit{C}\mathrm{H_2OH}$), 27.4 (s, $\mathrm{P}\mathit{C}\mathrm{H_2(CH_2)_2CH_3}$), 26.1 (s, $\mathrm{PCH_2}\mathit{C}\mathrm{H_2CH_2CH_3}$), 24.8 (d, $^3J_{\mathrm{C,P}}$ = 9 Hz, $\mathrm{P(CH_2)_2}\mathit{C}\mathrm{H_2CH_3}$), 13.9 (s, $\mathrm{P(CH_2)_3}\mathit{C}\mathrm{H_3}$). **^{31}P{^{1}H} NMR** ($\mathrm{CDCl_3}$): δ −20.3.

4.3.2.7. *$[Cu(PBu_3)_3(S_2CN(CH_2CH{=}CH_2)_2)]$* (***6c***). Yield: 775 mg (0.92 mmol, 92% based on **1c**). *Anal.* Calc. for $C_{43}H_{91}CuNP_3S_2$ (842.79): C, 61.28; H, 10.88; N, 1.66. Found: C, 60.81; H, 10.95; N, 1.60%. **IR** (NaCl): 3360 (O–H); 2960, 2869 (C–H); 1464 (C–N); 1095 (C–S) cm^{-1}. **^{1}H NMR** ($CDCl_3$): δ 5.88–5.81 (m, NCH_2CHCH_2, 2H), 5.11 (ddd, $^3J_{H,H}$ = 6 Hz, $^3J_{H,H}$ = 6 Hz, $^3J_{H,H}$ = 6 Hz, NCH_2CHCH_2, 4H), 4.53 (d, $^3J_{H,H}$ = 6 Hz, NCH_2CHCH_2, 4H), 1.50–1.40 (m, $P(CH_2)_2CH_2CH_3$, 36H), 1.38–1.31 (m, $P(CH_2)_2CH_2CH_3$, 18H), 0.87 (t, $^3J_{H,H}$ = 7 Hz, $P(CH_2)_3CH_3$, 27H). **^{13}C{^{1}H} NMR** ($CDCl_3$): δ 210.7 (s, S_2CN), 133.0 (s, NCH_2CHCH_2), 116.7 (s, NCH_2CHCH_2), 53.2 (s, NCH_2CHCH_2), 27.3 (s, $PCH_2(CH_2)_2CH_3$), 26.1 (s, $PCH_2CH_2CH_2CH_3$), 25.8 (d, $^3J_{C,P}$ = 7 Hz, $P(CH_2)_2CH_2CH_3$), 13.9 (s, $P(CH_2)_3CH_3$). **^{31}P{^{1}H} NMR** ($CDCl_3$): δ −20.1.

4.3.2.8. *$[Cu(PBu_3)_3(S_2CN(CH_2)_4)]$* (***6d***). Yield: 720 mg (0.88 mmol, 88% based on **1c**). *Anal.* Calc. for $C_{41}H_{89}CuNP_3S_2$ (816.75): C, 60.29; H, 10.98; N, 1.71. Found: C, 60.30; H, 11.20; N, 1.60%. **IR** (NaCl): 3378 (O–H); 2960, 2870 (C–H); 1458 (C–N); 1096 (C–S) cm^{-1}. **^{1}H NMR** ($CDCl_3$): δ 3.68 (t, $^3J_{H,H}$ = 7 Hz, C^3H_2,C^4H_2/$N(CH_2)_4$, 4H), 1.90–1.85 (m, C^2H_2,C^5H_2/$N(CH_2)_4$, 4H), 1.43–1.27 (m, $P(CH_2)_3CH_3$, 54H), 0.83 (t, $^3J_{H,H}$ = 7 Hz, $P(CH_2)_3CH_3$, 27H). **^{13}C{^{1}H} NMR** ($CDCl_3$): δ 205.2 (s, S_2CN), 51.3 (s, C^2,C^5/$N(CH_2)_4$), 27.2 (s, $PCH_2(CH_2)CH_3$), 26.1 (s, C^3,C^4/$N(CH_2)_4$), 26.0 (s, $PCH_2CH_2CH_2CH_3$), 24.7 (d, $^3J_{C,P}$ = 10 Hz, $P(CH_2)_2CH_2CH_3$), 13.8 (s, $P(CH_2)_3CH_3$). **^{31}P{^{1}H} NMR** ($CDCl_3$): δ −22.3.

4.3.2.9. *$[Ag(PBu_3)(S_2CNMe(C_2H_4OH))]$ (7).* Yield: 425 mg (0.92 mmol, 92% based on **2a**). *Anal.* Calc. for $C_{16}H_{35}AgNOPS_2$ (460.43): C, 41.74; H, 7.66; N, 3.04. Found: C, 41.27; H, 7.60; N, 2.82%. **IR** (NaCl): 3390 (O–H); 2925, 2870 (C–H); 1463 (C–N); 1099 (C–S) cm^{-1}. **^{1}H NMR** ($CDCl_3$): δ 4.24 (t, $^3J_{HH}$ = 5 Hz, NCH_2CH_2OH, 2H), 3.94 (dd, $^3J_{HH}$ = 9 Hz, $^3J_{HH}$ = 7 Hz, NCH_2CH_2OH, 2H), 3.49 (s, NCH_3, 3H), 3.40 (bs, OH, 1H), 1.57–1.33 (m, $PCH_2(CH_2)_2CH_3$, 18H), 0.90 (t, $^3J_{HH}$ = 7 Hz, $P(CH_2)_3CH_3$, 9H). **^{13}C{^{1}H} NMR** ($CDCl_3$): δ 212.9 (s, S_2CN), 62.0 (s, NCH_2CH_2OH), 58.2 (s, NCH_2CH_2OH), 43.4 (s, NCH_3), 27.6 (s, $PCH_2(CH_2)_2CH_3$), 25.9 (d, $^2J_{P-C}$ = 8 Hz, $PCH_2CH_2CH_2CH_3$), 24.7 (d, $^3J_{P-C}$ = 12 Hz, $P(CH_2)_2CH_2CH_3$), 13.9 (s, $P(CH_2)_3CH_3$). **^{31}P{^{1}H} NMR** ($CDCl_3$): δ −6.3.

4.3.2.10. *$[Ag(PBu_3)_2(S_2CNMe(C_2H_4OH))]$* (***8a***). Yield: 605 mg (0.91 mmol, 91% based on **2b**). *Anal.* Calc. for $C_{28}H_{62}AgNOP_2S_2$ (662.74): C, 50.74; H, 9.43; N, 2.11. Found: C, 50.30; H, 9.38; N, 2.02%. **IR** (NaCl): 3371 (O–H); 2955, 2928, 2870 (C–H); 1463 (C–N); 1097 (C–S) cm^{-1}. **^{1}H NMR** ($CDCl_3$): δ 4.25 (t, $^3J_{HH}$ = 5 Hz, NCH_2CH_2OH, 2H), 3.93 (p.q (dt), $^3J_{HH}$ = 5 Hz, $^3J_{HH}$ = 5 Hz, NCH_2CH_2OH, 2H), 3.51 (s, NCH_3, 3H), 3.37 (bs, OH, 1H), 1.60–1.56 (m, $PCH_2(CH_2)_2CH_3$, 12H), 1.52–1.44 (m, $PCH_2CH_2CH_2CH_3$, 12H), 1.42–1.35 (m, $P(CH_2)_2CH_2CH_3$, 12H), 0.90 (t, $^3J_{HH}$ = 7 Hz, $P(CH_2)_3CH_3$, 18H). **^{13}C{^{1}H} NMR** ($CDCl_3$): δ 213.0 (s, S_2CN), 62.1 (s, NCH_2CH_2OH), 58.1 (s, NCH_2CH_2OH), 43.3 (s, NCH_3), 27.7 (d, $^1J_{P-C}$ = 6 Hz, $PCH_2(CH_2)_2CH_3$), 26.0 (d, $^2J_{P-C}$ = 10 Hz, $PCH_2CH_2CH_2CH_3$), 24.7 (d, $^3J_{P-C}$ = 13 Hz, $P(CH_2)_2CH_2CH_3$), 13.9 (s, $P(CH_2)_3CH_3$). **^{31}P{^{1}H} NMR** ($CDCl_3$): δ −9.6.

4.3.2.11. *$[Ag(PBu_3)_2(S_2CN(CH_2CH{=}CH_2)_2)]$ (8b).* Yield: 603 mg (0.88 mmol, 88% based on **2b**). *Anal.* Calc. for $C_{31}H_{64}AgNP_2S_2$ (684.79): C, 54.37; H, 9.42; N, 2.05. Found: C, 54.34; H, 9.60; N, 1.91%. **IR** (NaCl): 3392 (O–H); 2959, 2930, 2871 (C–H); 1464 (C–N); 1095 (C–S) cm^{-1}. **^{1}H NMR** ($CDCl_3$): δ 5.94–5.87 (m, NCH_2CHCH_2, 2H), 5.13 (dd, $^3J_{H,H}$ = 4 Hz, $^3J_{H,H}$ = 11 Hz, NCH_2CHCH_2, 4H), 4.63 (d, $^3J_{H,H}$ = 5 Hz, NCH_2CHCH_2, 4H), 1.60–1.55 (m, $PCH_2CH_2CH_2CH_3$, 12H), 1.52–1.45 (m, $PCH_2CH_2CH_2CH_3$, 12H), 1.42–1.36 (m, $PCH_2CH_2CH_2CH_3$, 12H), 0.89 (t, $^3J_{H,H}$ = 7 Hz, $P(CH_2)_3CH_3$, 18H). **^{13}C{^{1}H} NMR** ($CDCl_3$): δ 212.5 (s, S_2CN), 133.1 (s, NCH_2CHCH_2), 116.8 (s, NCH_2CHCH_2), 55.2 (s, NCH_2CHCH_2), 27.7 (d, $^1J_{C,P}$ = 6 Hz, $PCH_2(CH_2)_2CH_3$), 26.1 (d, $^2J_{C,P}$ = 10 Hz, $PCH_2CH_2CH_2CH_3$), 24.7 (d, $^3J_{C,P}$ = 13 Hz, $P(CH_2)_2CH_2CH_3$), 13.9 (s, $P(CH_2)_3CH_3$). **^{31}P{^{1}H} NMR** ($CDCl_3$): δ −9.9.

4.3.2.12. *$[Ag(PBu_3)_3(S_2CNMe(C_2H_4OH))]$* (***9a***). Yield: 795 mg (0.92 mmol, 92% based on **2c**). *Anal.* Calc. for $C_{40}H_{89}AgNOP_3S_2$ (865.06): C, 55.54; H, 10.37; N, 1.62. Found: C, 55.48; H, 10.30; N, 1.53%. **IR** (NaCl): 3384 (O–H); 2957, 2928, 2871 (C–H); 1465 (C–N); 1099 (C–S) cm^{-1}.**^{1}H NMR** ($CDCl_3$): δ 4.27 (t, $^3J_{H,H}$ = 5 Hz, NCH_2CH_2OH, 2H), 3.92 (dd, $^3J_{H,H}$ = 10 Hz, $^3J_{H,H}$ = 5 Hz, NCH_2CH_2OH, 2H), 3.58 (t, $^3J_{H,H}$ = 5 Hz, OH, 1H), 3.50 (s, NCH_3, 3H), 1.52–1.34 (m, $PCH_2CH_2CH_2CH_3$, 54H), 0.90 (t, $^3J_{H,H}$ = 7 Hz, $P(CH_2)_3CH_3$, 27H). **^{13}C{^{1}H} NMR** ($CDCl_3$): δ 213.2 (s, S_2CN), 62.3 (s, NCH_2CH_2OH), 57.8 (s, NCH_2CH_2OH), 43.0 (s, NCH_3), 27.9 (d, $^1J_{C,P}$ = 8 Hz, $PCH_2(CH_2)_2CH_3$), 26.4 (d, $^2J_{C,P}$ = 2 Hz, $PCH_2CH_2CH_2CH_3$), 24.7 (d, $^3J_{C,P}$ = 12 Hz, $P(CH_2)_2CH_2CH_3$), 14.0 (s, $P(CH_2)_3CH_3$). **^{31}P{^{1}H} NMR** ($CDCl_3$): δ −17.7.

4.3.2.13. *$[Ag(PBu_3)_3(S_2CN(CH_2CH{=}CH_2)_2)]$* (***9b***). Yield: 590 mg (0.86 mmol, 86% based on **2c**). *Anal.* Calc. for $C_{43}H_{91}AgNP_3S_2$ (887.11): C, 58.22; H, 10.34; N, 1.58. Found: C, 57.84; H, 10.19; N, 1.57%. **IR** (NaCl): 3393 (O–H); 2954, 2931, 2872 (C–H); 1464 (C–N); 1095 (C–S) cm^{-1}. **^{1}H NMR** ($CDCl_3$): δ 5.90–5.83 (m, NCH_2CHCH_2, 2H), 5.07 (dd, $^3J_{H,H}$ = 8 Hz, $^3J_{H,H}$ = 9 Hz, NCH_2CHCH_2, 4H), 4.59 (d, $^3J_{H,H}$ = 5 Hz, NCH_2CHCH_2, 4H), 1.50–1.30 (m, $PCH_2CH_2CH_2CH_3$, 54H), 0.85 (t, $^3J_{H,H}$ = 7 Hz, $P(CH_2)_3CH_3$, 27H). **^{13}C{^{1}H} NMR** ($CDCl_3$): δ 212.4 (s, S_2CN), 133.2 (s, NCH_2CHCH_2), 116.3 (s, NCH_2CHCH_2), 54.7 (s, NCH_2CHCH_2), 27.6 (d, $^1J_{C,P}$ = 8 Hz, $PCH_2(CH_2)_2CH_3$), 26.1 (d, $^2J_{C,P}$ = 4 Hz, $PCH_2CH_2CH_2CH_3$), 24.5 (d, $^3J_{C,P}$ = 13 Hz, $P(CH_2)_2CH_2CH_3$), 13.8 (s, $P(CH_2)_3CH_3$). **^{31}P{^{1}H} NMR** ($CDCl_3$): δ −15.9.

4.3.3. Synthesis of bis(triphenylphosphine) silver(I) dithiocarbamates *12a,b*

Complex $[AgS_2CNR(C_2H_4OH)]$ (**11a**, R = Me; **11b**, R = Bu) (1.0 mmol) was suspended in dichloromethane (50 mL) and PPh_3 (2.0 mmol) was added in a single portion. After stirring this suspension at ambient temperature for 4 h, filtration through a pad of Celite and evaporation of the solvent in *oil-pump* vacuum gave **12a,b** as off-white solids.

4.3.3.1. *$[Ag(PPh_3)_2S_2CNMe(C_2H_4OH)]$* (***12a***). Yield: 730 mg (0.93 mmol, 93% based on **11a**). **Mp**: 170 °C. *Anal.* Calc. for $C_{40}H_{38}AgNOP_2S_2$ (782.68): C, 61.38; H, 4.89; N, 1.79. Found: C, 61.03; H, 4.99; N, 1.67%. **IR** (KBr): 3400 (O–H); 3069, 3055, 3015, 3000, 2964, 2924, 2859 (C–H); 1479 (C–N); 1094 (C–S) cm^{-1}. **^{1}H NMR** ($CDCl_3$): 7.34–7.29 (m, C_6H_5, 12H), 7.28–7.24 (m, C_6H_5, 6H), 7.22–7.17 (m, C_6H_5, 12H), 4.11 (t, $^3J_{HH}$ = 5 Hz, NCH_2CH_2OH, 2H), 3.87 (p.q, $^3J_{HH}$ = 6 Hz, CH_2CH_2OH, 2H), 3.44 (s, NCH_3, 3H). **^{13}C{^{1}H} NMR** ($CDCl_3$): δ signal for S_2CN not found, 134.4 (d, J_{CP} = 15 Hz, C^i/C_6H_5), 134.0 (d, $^2J_{CP}$ = 17 Hz, C^o/C_6H_5), 129.7 (C^p/C_6H_5), 128.7 (d, $^3J_{CP}$ = 9 Hz, C^m/C_6H_5), 61.5 (s, NCH_2CH_2OH), 58.5 (s, NCH_2CH_2OH), 44.3(s, NCH_3). **^{31}P{^{1}H} NMR** ($CDCl_3$): δ 4.8.

4.3.3.2. *$[Ag(PPh_3)_2S_2CNBu(C_2H_4OH)]$* (***12b***). Yield: 790 mg (0.96 mmol, 96% based on **11b**). **Mp**: 161 °C. *Anal.* Calc. for $C_{43}H_{44}AgNOP_2S_2$ (824.76): C, 62.62; H, 5.38; N, 1.70. Found: C, 62.13; H, 5.32; N, 1.75%. **IR** (KBr): 3388 (O–H); 3067, 3057, 3013, 3002, 2953, 2928, 2867 (C–H); 1481 (C–N); 1111 (C–S) cm^{-1}. **^{1}H NMR** ($CDCl_3$): δ 7.42–7.38 (m, C_6H_5, 12H), 7.37–7.33 (m, C_6H_5, 6H), 7.31–7.27 (m, C_6H_5, 12H), 4.17 (t, $^3J_{HH}$ = 5.4 Hz, NCH_2CH_2OH, 2 H), 4.01–3.97 (m, NCH_2CH_2OH/$CH_2(CH_2)_2CH_3$, 4H), 2.92 (t, $^3J_{HH}$ = 5.7 Hz, OH, 1H), 1.79–1.73 (m, $CH_2CH_2CH_2CH_3$, 2H), 1.36–1.28 (m, $CH_2CH_2CH_2CH_3$, 2H), 0.92 (t, $^3J_{HH}$ = 7.4 Hz, $CH_2CH_2CH_2CH_3$, 3H). **^{13}C{^{1}H} NMR** ($CDCl_3$): δ 211.2 (s, S_2CN), 134.4 (d, J_{CP} = 15 Hz, C^i/C_6H_5), 134.1 (d, $^2J_{CP}$ = 17 Hz, C^o/C_6H_5), 129.7 (C^p/C_6H_5), 128.8 (d, $^3J_{CP}$ = 9 Hz, C^m/C_6H_5), 61.5 (s, NCH_2CH_2OH), 56.4/56.1 (s/s,

$NCH_2\mathit{C}H_2OH/N\mathit{C}H_2(CH_2)_2CH_3$), 29.2 (s, $NCH_2\mathit{C}H_2CH_2CH_3$), 20.3 (s, $N(CH_2)_2\mathit{C}H_2CH_3$), 14.0 (s, $N(CH_2)_3\mathit{C}H_3$). **$^{31}P\{^1H\}$ NMR** ($CDCl_3$): δ 4.9.

4.3.4. Single crystal X-ray diffraction analysis

Single crystals of **12a**,**b** suitable for X-ray diffraction analysis were obtained by diffusion of diethyl ether into a saturated dichloromethane solution containing the respective compound. Data were collected with an Oxford Gemini S diffractometer at 117 (**12a**) and 100 K (**12b**) using Cu Kα radiation (λ = 1.54184 Å). The structures were solved solved by direct methods and refined by full-matrix least-squares procedures on F^2. [24] All *non*-hydrogen atoms were refined anisotropically, and a riding model was employed in the treatment of the hydrogen atom positions.

***12b**:* The OH group and the additional solvent molecule CH_2Cl_2 are disordered and have been refined to split occupancies of 0.52/0.48 (O1, C8, Cl1, Cl2).

*4.3.4.2. Crystal data for **12a**·CH_2Cl_2.* $C_{41}H_{40}AgCl_2NOP_2S_2$, M = 867.57 g mol^{-1}, T = 117 K, λ = 1.54184 Å, triclinic, $P\bar{1}$, a = 12.2750(7) Å, b = 13.0674(7) Å, c = 13.9428(9) Å, α = 98.401(5)°, β = 93.825(5)°, γ = 116.357(6)°, V = 1960.5(2) Å^3, ρ_{calc} = 1.470 g cm^{-3}, $F(000)$ = 888, crystal dimensions 0.36 × 0.18 × 0.14 mm, Z = 2, minimum/maximum transmission: 1.00000/0.66015, μ = 7.403 mm^{-1}, θ range = 3.24–63.96°, Index ranges $-8 \leqslant h \leqslant 14$, $-14 \leqslant k \leqslant 15$, $-16 \leqslant l \leqslant 14$, total/unique reflections: 10960/6359, data/restraints/parameters: 6359/0/451, R_{int} = 0.0329, R_1 = 0.0410, wR_2 = 0.1041 [$I > 2\sigma(I)$], R_1 = 0.0453, wR_2 = 0.1058 [all data], completeness to θ_{max}: 97.8%/63.96°, Goodness-of-fit S on F^2: 0.987, largest difference in peak/hole: 1.127/−0.781 eÅ^{-3}.

*4.3.4.3. Crystal data for **12b**·CH_2Cl_2.* $C_{44}H_{46}AgCl_2NOP_2S_2$, M = 909.65 g mol^{-1}, T = 100 K, λ = 1.54184 Å, triclinic, $P\bar{1}$, a = 12.5600(5) Å, b = 13.0691(7) Å, c = 14.4305(8) Å, α = 96.482(5)°, β = 93.827(4)°, γ = 116.739(5)°, V = 2083.39(18) Å^3, ρ_{calc} = 1.450 g cm^{-3}, $F(000)$ = 936, crystal dimensions 0.22 × 0.14 × 0.03 mm, Z = 2, minimum/maximum transmission: 1.00000/0.43895, μ = 6.993 mm^{-1}, θ range = 3.11°–65.48°, Index ranges $-14 \leqslant h \leqslant 14$, $-13 \leqslant k \leqslant 15$, $-16 \leqslant l \leqslant 17$, total/unique reflections: 11958/7019, data/restraints/parameters: 7019/52/504, R_{int} = 0.0277, R_1 = 0.0442, wR_2 = 0.1139 [$I > 2\sigma(I)$], R_1 = 0.0523, wR_2 = 0.1166 [all data], completeness to θ_{max}: 97.8%/65.48°, Goodness-of-fit S on F^2: 0.966, largest difference in peak/hole: 1.403/−0.784 eÅ^{-3}.

Acknowledgments

We are grateful to the Deutsche Forschungsgemeinschaft (IRTG, Materials and Concepts for Advanced Interconnects, GRK 1215) for generous financial support. We acknowledge Prof. Michael Mehring and Dr. Maik Schlesinger for XRPD measurements.

Appendix A. Supplementary material

CCDC 1032495 and 1032496 contain the supplementary crystallographic data for **12a** and **12b** respectively. These data can be obtained free of charge from The Cambridge Crystallographic Data Centre via www.ccdc.cam.ac.uk/data_request/cif. Supplementary data associated with this article can be found, in the online version, at http://dx.doi.org/10.1016/j.ica.2015.02.008.

References

[1] G. Hogarth, Transition Metal Dithiocarbamates: 1978–2003, in Progress in Inorganic Chemistry, Volume 53 (Ed. K. D. Karlin), 2005, John Wiley & Sons Inc, Hoboken, NJ, USA and references cited therein.
[2] (a) A.A. Ensafi, S. Abbasi, Anal. Sci. 16 (2000) 377;
(b) M.K. Deb, S. Chakravarty, R.K. Mishra, J. Indian Chem. Soc. 73 (1996) 551;
(c) M. Sperling, X.F. Yin, B. Welz, Analyst 117 (1992) 629;
(d) A.K. Malik, A.L.J. Rao, J. Chin. Chem. Soc. 39 (1992) 235.
[3] (a) H.S. Sangari, G.S. Sodhi, J. Kaur, Thermochim. Acta 171 (1990) 49;
(b) P. O'Brien, J.H. Park, J. Waters, Thin Solid Films 431 (2003) 502;
(c) R. Nomura, H. Matsuda, Trends Inorg. Chem. 2 (1991) 79;
(d) C. Bernal, E.A. Neves, E.T.G. Cavalhiero, Thermochim. Acta 370 (2001) 49;
(e) M. Kemmler, M. Lazell, P. O'Brien, D.J. Otway, J.H. Park, J.R. Walsh, J. Mater. Sci. Mater. Electron. 13 (2002) 531.
[4] (a) Z.-Q. Wang, S.-W. Lu, H.-F. Guo, N.-H. Hu, Polyhedron 11 (1992) 1131;
(b) A. Srivastava, Y.A. Ma, R. Pankayatselvan, W. Dinges, K.M. Nicholas, J. Chem. Soc., Chem. Commun. 853 (1992) 42.
[5] (a) R. Ramesh, K. Natarajan, Synth. React. Inorg. Met. Org. Chem. 26 (1996) 1677;
(b) D.G. Craciunescu, C. Molina, A. Doadrio-López, E. Parrondo-Iglesias, A. Gomez, M. Sanchez de Leon, L. Fernandez de Simon, E. Gastón de Iriarte, C. Guirvu, An. R. Acad. Farm 53 (1987) 205.
[6] G. Exarchos, S.D. Robinson, J.W. Steed, Polyhedron 20 (2001) 2951.
[7] H. Zhu, X. Zhang, B. Zuo, Hebei Daxue Xuebao, Ziran Kexueban 16 (1996) 58.
[8] (a) C. Di Nicola, J. Ngoune, Effendy, C. Pettinari, B.W. Skelton, A.H. White, Inorg. Chim. Acta 360 (2007) 2935;
(b) A.H. Othman, H.-K. Fun, K. Sivakumar, Acta Crystallogr., Sect. C 52 (1996) 843;
(c) M.C. Gimeno, P.G. Jones, A. Laguna, C. Sarroca, Polyhedron 17 (1998) 3681;
(d) V. Venkatachalam, K. Ramalingam, Synth. React. Inorg. Met. Org. Chem. 26 (1996) 112.
[9] (a) Ö. Güzel, A. Salman, Bioorg. Med. Chem. 14 (2006) 7804;
(b) S. Ozkirimli, T.I. Apak, M. Kiraz, Y. Yegenoglu, Arch. Pharm. Res. 28 (2005) 1213.
[10] F. Bonati, R. Udo, J. Organomet. Chem. 10 (1967) 257.
[11] R. Kellner, G.S. Nikolov, N. Trendafilova, Inorg. Chim Acta 84 (1984) 233.
[12] H. Friebolin, G. Schilling, L. Pohl, Org. Magn. Reson. 12 (1979) 569.
[13] S.M. Socol, R.A. Jacobson, J.G. Verkade, Inorg. Chem. 23 (1984) 88.
[14] (a) U. Siegert, H. Hahn, H. Lang, Inorg. Chim. Acta 363 (2010) 944;
(b) E.L. Muetterties, C.W. Alegranti, J. Am. Chem. Soc. 92 (1970) 4114;
(c) E.L. Muetterties, C.W. Alegranti, J. Am. Chem. Soc. 94 (1972) 6386;
(d) Z. Yuan, N.H. Dryden, J.J. Vittal, R.J. Puddephatt, Chem. Mater. 7 (1995) 1696;
(e) R.G. Goel, P. Pilon, Inorg. Chem. 17 (1978) 2876.
[15] R. Mothes, Y. Shen, A. Jakob, B. Walfort, T. Rüffer, S.E. Schulz, R. Ecke, T. Gessner, H. Lang, Dalton Trans. 39 (2010) 11235.
[16] M.D. Gordon, L.D. Quin, J. Magn. Reson. 22 (1976) 149.
[17] S. Berger, S. Braun, H.-O. Kalinowski, (1992) in NMR-Spektroskopie von Nichtmetallen, Vol. 2, G. Thieme Verlag, Stuttgart, Engl Ed., Wiley VCH Verlag GmbH, Weinheim.
[18] A.H. Othman, H.-K. Fun, K. Sivakumar, Acta Crystallogr., Sect. C 52 (1996) 843.
[19] (a) R. Nomura, M. Kori, H. Matsuda, Chem. Lett. (1985) 579;
(b) R. Nomura, K. Kanaya, H. Matsuda, Ind. Eng. Chem. Res. 28 (6) (1989) 877.
[20] R. Mothes, A. Jakob, T. Waechtler, S. E. Schulz, T. Geßner, H. Lang, Eur. J. Inorg. Chem. submitted. http://dx.doi.org/10.1002/ejic.201403182
[21] (a) A. Grodzicki, I. Łakomska, P. Piszczek, I. Szymańska, E. Szłyk, Coord. Chem. Rev. 249 (2005) 2232;
(b) A. Jakob, Y. Shen, T. Wächtler, S.E. Schulz, T. Gessner, R. Riedel, C. Fasel, H. Lang, Z. Anorg. Allg. Chem. 634 (12–13) (2008) 2226. and references cited therein.
[22] (a) E.W. Tyler III, M.B. Dines, US Patent no. 3776972, 1973. (b) E.W. Tyler III, M.B. Dines, US Patent no. 3933878, 1976.
[23] K. Okumura, S. Kouyama, J. Photopolym. Sci. Technol. 8 (3) (1995) 365.
[24] (a) G.M. Sheldrick, Acta Crystallogr., Sect. A 46 (1990) 467;
(b) G.M. Sheldrick, SHELXL-97 Program for Crystal Structure Refinement, Universität Göttingen, 1997.